Original Article

The effects of the oral administration of graphene oxide on the gut microbiota and ultrastructure of the colon of mice

Jiamen Shen[1#]^, Jiatian Dong[1#], Jiaying Zhao[1], Tao Ye[1], Lifeng Gong[1], Huipeng Wang[1], Wenjie Chen[1], Mingsheng Fu[2*], Yuankun Cai[1*]^

[1]Department of General Surgery, The Fifth People's Hospital of Shanghai, Fudan University, Shanghai, China; [2]Department of Gastroenterology, The Fifth People's Hospital of Shanghai, Fudan University, Shanghai, China

Contributions: (I) Conception and design: J Shen, J Dong, M Fu, Y Cai; (II) Administrative support: Y Cai; (III) Provision of study materials or patients: J Shen, M Fu; (IV) Collection and assembly of data: J Shen, J Dong, H Wang, W Chen; (V) Data analysis and interpretation: J Shen, J Dong, J Zhao, T Ye, L Gong; (VI) Manuscript writing: All authors; (VII) Final approval of manuscript: All authors.

[#]These authors contributed equally to this work.

[*]These authors contributed equally to this work and should be considered as co-corresponding authors.

Correspondence to: Yuankun Cai. Department of General Surgery, The Fifth People's Hospital of Shanghai, Fudan University, No. 801 Heqing Road, Shanghai 200240, China. Email: yuankun@medmail.com.cn; Mingsheng Fu. Department of Gastroenterology, The Fifth People's Hospital of Shanghai, Fudan University, No. 801 Heqing Road, Shanghai 200240, China. Email: fumingsheng@fudan.edu.cn.

Background: Graphene oxide (GO) has been widely used in the field of biomedicine and has shown great potential in drug delivery. Oral administration is an important mode of administration, but there are few studies on the effects of oral GO on gastrointestinal tract and gut microbiota. This study sought to explore the effects of oral GO on the gastrointestinal tract and gut microbiota.

Methods: In total, 20 C57BL/6 male mice, aged 5 weeks old, were randomly divided into the following 4 groups (n=5): the control group, the GO30 group, the GO60 group, and the GO120 group. The GO sample solution was administered intragastrically at the doses of 30, 60, or 120 mg/kg every 3 days, and the control group was given an equal volume of distilled water. On the 16th day, mouse feces were taken for 16S ribosomal ribonucleic acid (rRNA) sequencing analysis, and the mice were dissected, and the heart, liver, kidney, and colon removed for histological analysis. Additionally, the ultrastructure of the colon was observed by transmission electron microscopy.

Results: No obvious damage was observed in the hearts, livers, and kidneys of the mice. However, the intestinal ultrastructure of the mice in the GO group was damaged. The main manifestations were an uneven arrangement and local atrophy of the microvilli, swelling of the mitochondria and endoplasmic reticulum, and the widening of the intercellular spaces. The damage was positively correlated with increasing GO doses. The 16S rRNA sequencing results showed that the structure of the gut microbiota in the GO group was altered, and the contents of *Alistipes*, *Enterobacteriaceae*, *Eubacterium*, and *Xanthobacteraceae* were decreased.

Conclusions: The oral administration of GO had no obvious toxicity effects on the hearts, livers, and kidneys of the mice. However, it did destroy the ultrastructure of the mouse colon and shift the structure of the gut microbiota, decreasing the contents of *Alistipes*, *Enterobacteriaceae*, *Eubacterium*, and *Xanthobacteraceae*.

Keywords: Graphene oxide (GO); oral administration; gut microbiota

Submitted Jan 12, 2022. Accepted for publication Mar 10, 2022. This article was updated on September 25, 2024.
The original version is available at: http://dx.doi.org/10.21037/atm-22-922
doi: 10.21037/atm-22-922

^ ORCID: Jiamen Shen, 0000-0002-1148-1685; Yuankun Cai, 0000-0001-9735-200X.

Introduction

Graphene oxide (GO) is a honeycomb lattice-like 2-dimensional sheet composed of sp2 hybrid carbon atoms, with many oxygen-containing active groups on the surface, such as the carbonyl, hydroxyl, carboxyl, and epoxy groups (1). The lamellar structure and abundant oxygen-containing groups of GO determine its high specific surface area, good hydrophilicity, and easy modification (2-4). GO and its derivatives have been widely applied in many aspects of the biomedical field, such as the delivery of chemotherapy drugs (5-7), the preparation of antibacterial materials (8,9), biological imaging *in vivo* (10,11), dental pulp repair (12), and the photothermal treatment of tumors (13,14). And they have great potential to be applied in clinical practice. With the further application of GO, its biotoxicity and safety have become the focus of research. A study reported that nano-scale GO has a dose-dependent toxic effect on zebrafish embryonic development (15). Some scholars had found that the oral administration of GO nanoparticles causes various behavioral and developmental defects in the offspring of drosophila (16). A study based on human embryonic kidney cells also showed that GO has a significant dose-dependent cytotoxic effect on human embryonic kidney cells (17). Studies have found that the toxicity of GO and its derivatives are related to its surface coating, dose, particle size, and administration route, among which the administration route is the most critical, and oral administration has the highest safety (18,19). Additionally, a study on occupational exposure risk showed that the oral cavity is one of the main exposure routes of graphene-based materials (20). However, currently, very few studies have been conducted on the biological toxicity of oral GO, and its effects on the intestinal flora.

This study sought to examine the gastrointestinal toxicity of orally administrated GO, and its effects on gut microbiota. We present the following article in accordance with the ARRIVE reporting checklist (available at https://atm.amegroups.com/article/view/10.21037/atm-22-922/rc).

Methods

Preparation of GO by the modified-Hummers method

The modified-Hummers method was used to prepare the GO. The steps were as follows: graphite (4 g, 500 mesh) and concentrated sulfuric acid (25 mL) were mixed in a 500 mL beaker, and magnetically stirred for 1 h. Next, 2 g of sodium nitrate was added and stirred at 0 ℃ for 1 h, and 12 g of potassium permanganate was added slowly in batches; the temperature was kept below 5 ℃ during this process. The temperature was then increased to 35 ℃, and the stirring continued for 2 h. A total of 180 mL of deionized water was slowly added and stirred at 95 ℃ for 15 min. Hydrogen peroxide (20 mL, 30%) was slowly added, and washed with 1 mol/L hydrochloric acid dilute solution 3 times. Finally, dialysis was performed with an 8,000–12,000 D dialysis band for a week to obtain GO.

Animals and treatment

Animal experiments were carried out at the Experimental Animal Center of East China Normal University. In total, 20 C57BL/6 male mice (5 weeks old, 22–26 g) were purchased from the JSJ Laboratory Animal Technology Co., Ltd. (Shanghai, China). The mice were placed in a humidity-controlled room and subjected to a 12-h/12-h light-dark cycle, with free access to food and water. The mice were randomly divided into the following 4 groups (n=5): the control group, the GO30 group, the GO60 group, and the GO120 group. Every 3 days, the GO sample solution was administered by gavage at doses of 30, 60, or 120 mg/kg. The dose of GO is based on a previous report and our preliminary studies (18). The control group was given an equal volume of distilled water. The body weight of the mice was weighed and recorded every 3 days. Stool was collected on the 16th day, quickly frozen in liquid nitrogen, and then stored in a –80 ℃ refrigerator for subsequent analysis. Experiments were performed under a project license (No. m20210805) granted by Experimental Animal Welfare Ethics Committee of East China Normal University, in compliance with East China Normal University guidelines for the care and use of animals. A protocol was prepared before the study without registration.

Histological analysis

The mice were dissected for their organs 16 days later, and their colon, heart, liver, and kidney specimens were removed, fixed in 4% formaldehyde, embedded in paraffin, and sectioned at a thickness of about 4 μm. The sections were stained with hematoxylin-eosin (H&E) to observe the histological changes.

Transmission electron microscopy (TEM)

After the mice were dissected, the colon tissues of the mice

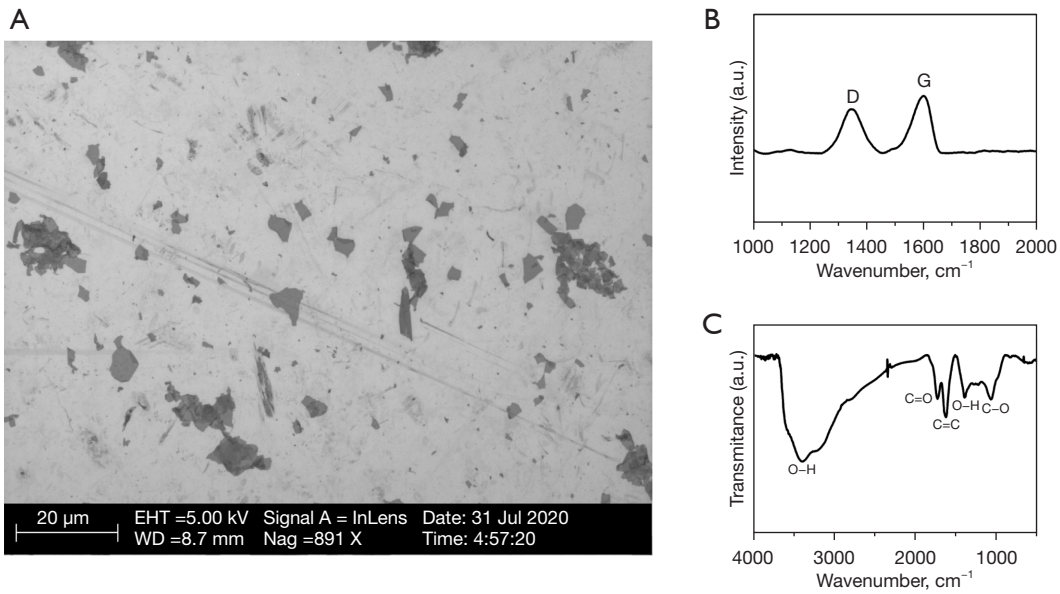

Figure 1 Characterization of GO. (A) SEM images. (B) GO Raman spectrum. (C) GO infrared spectrum. (B,C) were adapted from Shao *et al.* (21) with permission. D, D peak; G, G peak; GO, graphene oxide; SEM, scanning electron microscopy; EHT, extra high tension; WD, work distance.

were fixed with electron microscope fixative (Servicebio). Each sample size was about 1 mm^3. Next the sample was fixed with 1% osmium acid prepared by 0.1 M phosphate buffer (PB; pH 7.4) in the dark, at room temperature for 2 h, and rinsed 3 times with 0.1 M PB for 15 min each time. After the sample became dehydrated, EMBed 812 was used for resin penetration and embedding. The embedded resin sample was sliced and polymerized for 48 h in a 60 ℃ oven. Next, it was stained in a 2% uranium acetate saturated alcohol solution in the dark for 8 min, and in a 2.6% lead citrate without carbon dioxide for 8 min. After the sample dried, the images were observed and collected by TEM.

16S ribosomal ribonucleic acid (rRNA) gene sequencing

The16S rRNA gene sequencing was carried out by OE biotech Co., Ltd. (Shanghai, China). Fecal deoxyribonucleic acid (DNA) was extracted using the FastDNA® Stool rotation kit (MP Biomedical, SantaAna, USA), and amplified by V3-V4 variable region of the 16S rRNA gene. The polymerase chain reaction (PCR) was as follows: 5 min at 95 ℃, followed by 30 cycles at 95 ℃ for 30 s, 55 ℃ for 30 s, 72 ℃ for 30 s, and finally another 5 min at 72 ℃. The amplicon was frozen and purified using the QiaQuick PCR purification kit (Qiagen, Valencia, USA). The mixed PCR products were sequenced on the Illumina Miseq platform (SanDiego Illumina, USA) in accordance with the manufacturer's instructions.

Statistical analysis

The data are expressed as the mean ± standard deviation. R studio software was used for the statistical analysis. A one-way analysis of variance was conducted to analyze the differences among the 4 groups. A P value <0.05 was considered statistically different.

Results

Preparation of GO

Scanning electron microscopy (SEM) was used to observe the prepared GO. The GO was in the form of flakes with a diameter of 2 to 6 μm (see *Figure 1A*). The Raman spectrum (see *Figure 1B*) showed that the characteristic absorption peaks of GO at 1,345 and 1,601 cm^{-1} corresponded to peak D and peak G, respectively, and the ratio of peak D to peak G was 0.75. The infrared spectrum results showed that the prepared GO contained many oxygen-containing functional groups on the surface, such as carboxyl (-COOH), hydroxyl (-OH), and carbonyl (-CO) (see *Figure 1C*). The GO used in this study is from the same batch as that used in Shao *et al.* (21), and *Figure 1B,1C* was adapted from Shao *et al.* (21) with permission.

GO altered the ultrastructure of the colon in mice

As *Figure 2A* shows, the average weight of the mice in the GO120 group was significantly lower than that of the other groups. The difference between the other 3 groups was not statistically significant, but this suggested that the high dose of GO gavage reduced the weight of the mice. After the mice were dissected, the colon length of the GO120 group was found to be slightly shorter than that of the other 3 groups; however, the difference was not statistically significant (see *Figures 2B,2C*). The results of the H&E staining indicated that the hearts, livers, and kidneys of the mice in the 4 groups did not accumulate GO, or show any obvious damage (see *Figure 2D*).

The results of the H&E staining revealed no clear changes in the intestinal structure among the 4 groups, and no obvious colitis (see *Figure 3A*). However, the TEM results showed that there was damage to the ultrastructure of the mouse colon in the GO group (see *Figure 3B*). Notably, the injury was relatively serious in the GO120 group. Some cells had a tendency of apoptosis, but the cell membrane remained intact. The microvilli were arranged unevenly, sparsely, and shrunk locally. The epithelial cells showed obvious pyknosis, the organelles were swollen and aggregated, and the stroma showed pyknosis. The nucleus was irregularly shrunk, and the nuclear membrane expanded. The perinuclear space was widened, and the chromatin agglomerated. The mitochondria were abundant, and obviously swollen and enlarged. The local matrix was dissolved, and the cristae were fractured and decreased. Tight junctions were observed between the cells. The intercellular junctions were widened. The desmosomes decreased, and intercellular spaces were widened locally. The rough endoplasmic reticulum was obviously dilated, degranulated, and vacuolated.

GO shifted the structure of the gut microbiota

As *Figure 4A* shows, there was no significant difference in α diversity among the 4 groups, indicating that the degree of diversity in the 4 groups was similar. Next, a principal coordinate analysis (PcoA) map was constructed, and a Bray-Curtis distance analysis was performed to evaluate β diversity. The results showed that there were significant differences in β diversity (R^2=0.43874, P=0.017) among the 4 groups (see *Figure 4B,4C*). Next, the structural changes of the flora were analyzed at the phylum level and the genus level. At the phylum level, the structure of the flora among the 4 groups was very similar, but the content of GO120 firmicutes was significantly reduced (see *Figure 4D*). At the genus level, the structure of the flora among the 4 groups was also similar in general, but the composition of some of the flora was quite different, such as *Prevotellaceae*_UCG-001 and *Alistipes* (see *Figure 4E*).

Next, a *t*-test and the Lefse method [linear discriminant analysis (LDA) score >3] were used to evaluate the specific differences in community structure; the results are displayed in heat maps and bifurcations (see *Figure 5A,5B*). At the genus level, compared to the control group, GO significantly reduced *Xanthobacteraceae* (P<0.05), *Enterobacteriaceae* (P<0.05), *Eubacterium siraeum* (P<0.05), *Enterobacterales* (P<0.05) and the abundance of *Alistipes* (P<0.05) (see *Figure 5C*). To explore altered gut bacteria and their interaction, correlation network based on Spearman correlation analysis was constructed. The results showed that there were significant correlations among the bacteria from bacteroidota and firmicutes (see *Figure 6A*). The Kyoto Encyclopedia of Genes and Genomes (KEGG) enrichment analysis suggested that changes in gut microbiota caused by GO may affect the functions of cell movement, lipid metabolism, signal transduction, etc., but the difference was not statistically significant (see *Figure 6B*).

Discussion

GO is a novel nanomaterial with the advantages of a large specific surface area, hydrophilicity, and easy modification. It has been the focus of research since its discovery, and it has great potential in the field of biomedicine. GO was first introduced into the biomedical field as a chemotherapeutic drug carrier, and has been widely used in a variety of drug delivery systems (5-7). Additionally, it has also been applied in disease diagnosis (22), tumor photothermal treatment (13,14), tissue engineering (23), the preparation of antibacterial materials (8,9), and many other areas. Oral administration is one of the main routes of drug administration. As a drug carrier or dental restoration material, GO is inevitably taken into the body. However, very few studies have evaluated the toxicity of oral GO on the gastrointestinal tract, and its effects on the gut microbiota. Thus, this study explored the effects of GO on the gastrointestinal tract, and its effects on gut microbiota.

The results of the study showed that the body weight of the mice in the GO120 group was lower than that of mice in the other groups after the oral administration of GO, but the difference was not statistically significant. After

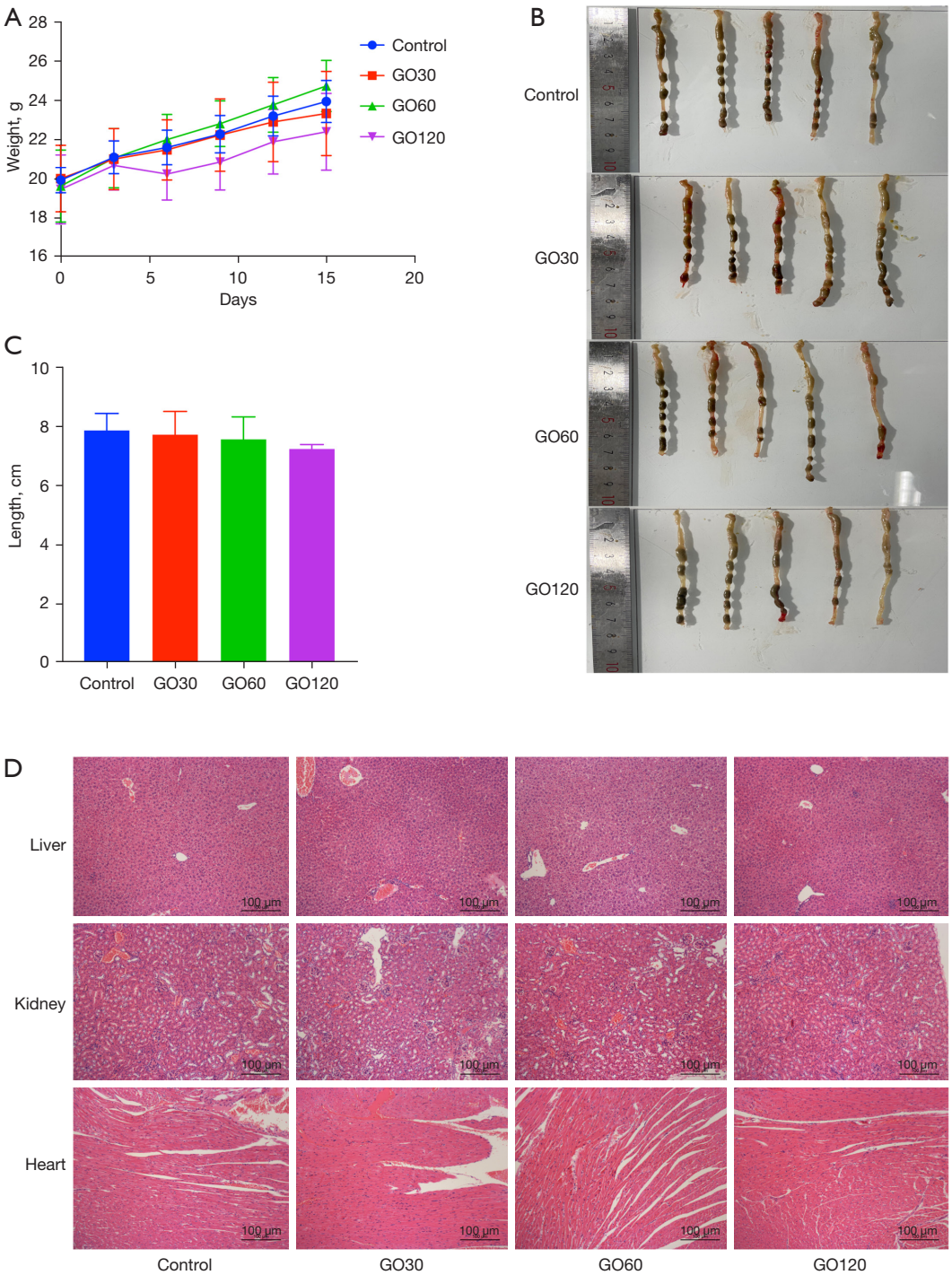

Figure 2 GO affects the body weight of mice, but has no obvious toxic effects on the heart, liver and kidney. (A) Body weight of mouse. (B) Gross specimen of mouse colon. (C) Length of colon. (D) H&E staining results of a mouse heart, liver, and kidney. GO30, group with GO of dose 30 mg/kg; GO60, group with GO of dose 60 mg/kg; GO120, group with GO of dose 120 mg/kg; GO, graphene oxide; H&E, hematoxylin-eosin.

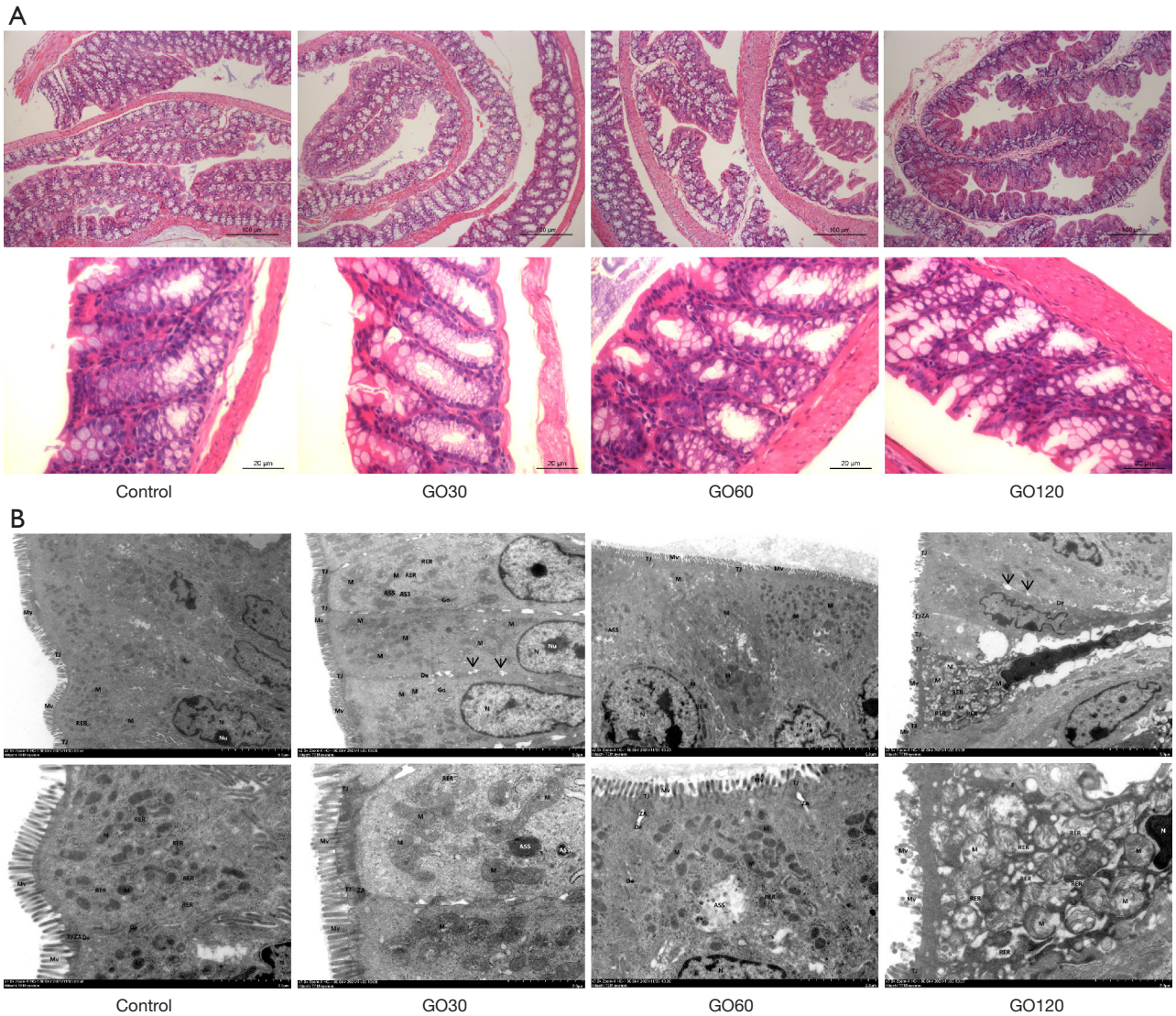

Figure 3 Ultrastructure of mouse colon damaged by GO. (A) H&E staining of a mouse colon. (B) TEM images of a mouse colon. Arrow: Widened intercellular space. GO30, group with GO of dose 30 mg/kg; GO60, group with GO of dose 60 mg/kg; GO120, group with GO of dose 120 mg/kg; GO, graphene oxide; ASS, autolysosome; De, desmosome; Go, Golgi apparatus; M, mitochondrion; Mv, microvillus; N, nucleus; Nu, nucleolus; RER, rough endoplasmic reticulum; TJ, tight junction; ZA, zonula adherens; TEM, transmission electron microscope.

the mice were dissected, it was found that the colon length of the GO120 group was slightly shorter than that of the mice in the other groups, but again, the difference was not statistically significant. The results of the H&E staining showed that there was no obvious GO absorption in the intestinal tissues of the mice, no obvious inflammatory responses in colon, and no obvious toxic effects in the hearts, livers, and kidneys of the mice, which indicated that the adsorption of GO in the intestines of mice was very limited. The results of this study are similar to those of Yang *et al.* (18).

The intestinal barrier is a barrier composed of a layer of closely connected intestinal mucosal epithelial cells and basement membrane. The main function of the intestinal barrier is to absorb water and nutrients, and act as a barrier to prevent harmful substances and microorganisms from migrating to other parts of the body. The disturbance of the intestinal barrier function is related to various

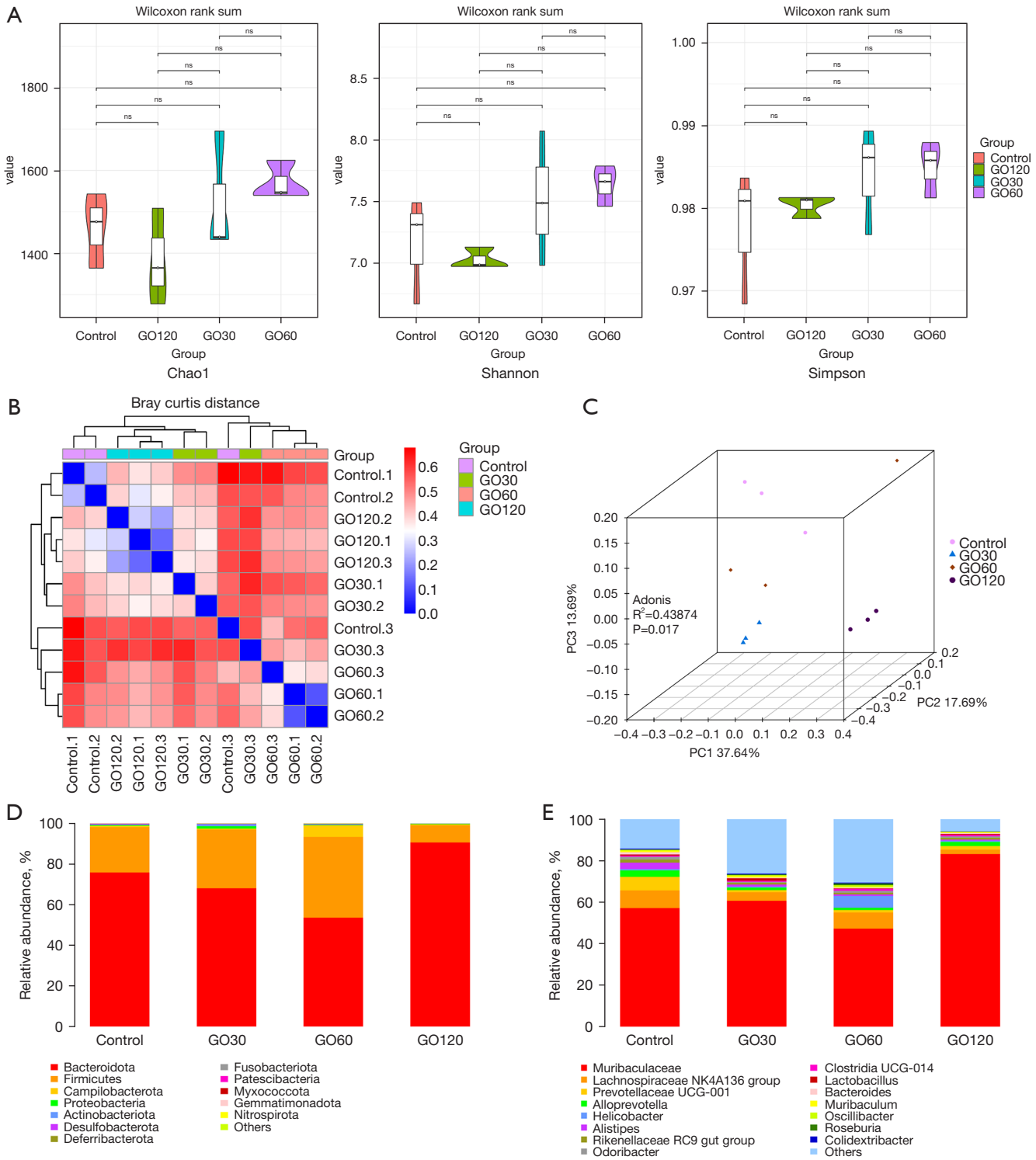

Figure 4 GO affects the diversity of the intestinal flora of mice. (A) α diversity of the 4 groups for gut microbes (the chao1 index, Shannon index, and Simpson index). (B) Bray-Curtis distance analysis. (C) β diversity index based on PCoA. (D,E) Relative intestinal microbial abundance at the phylum level and genus level. GO30, group with GO of dose 30 mg/kg; GO60, group with GO of dose 60 mg/kg; GO120, group with GO of dose 120 mg/kg; GO, graphene oxide; PCoA, principal coordinate analysis; ns, no significant difference.

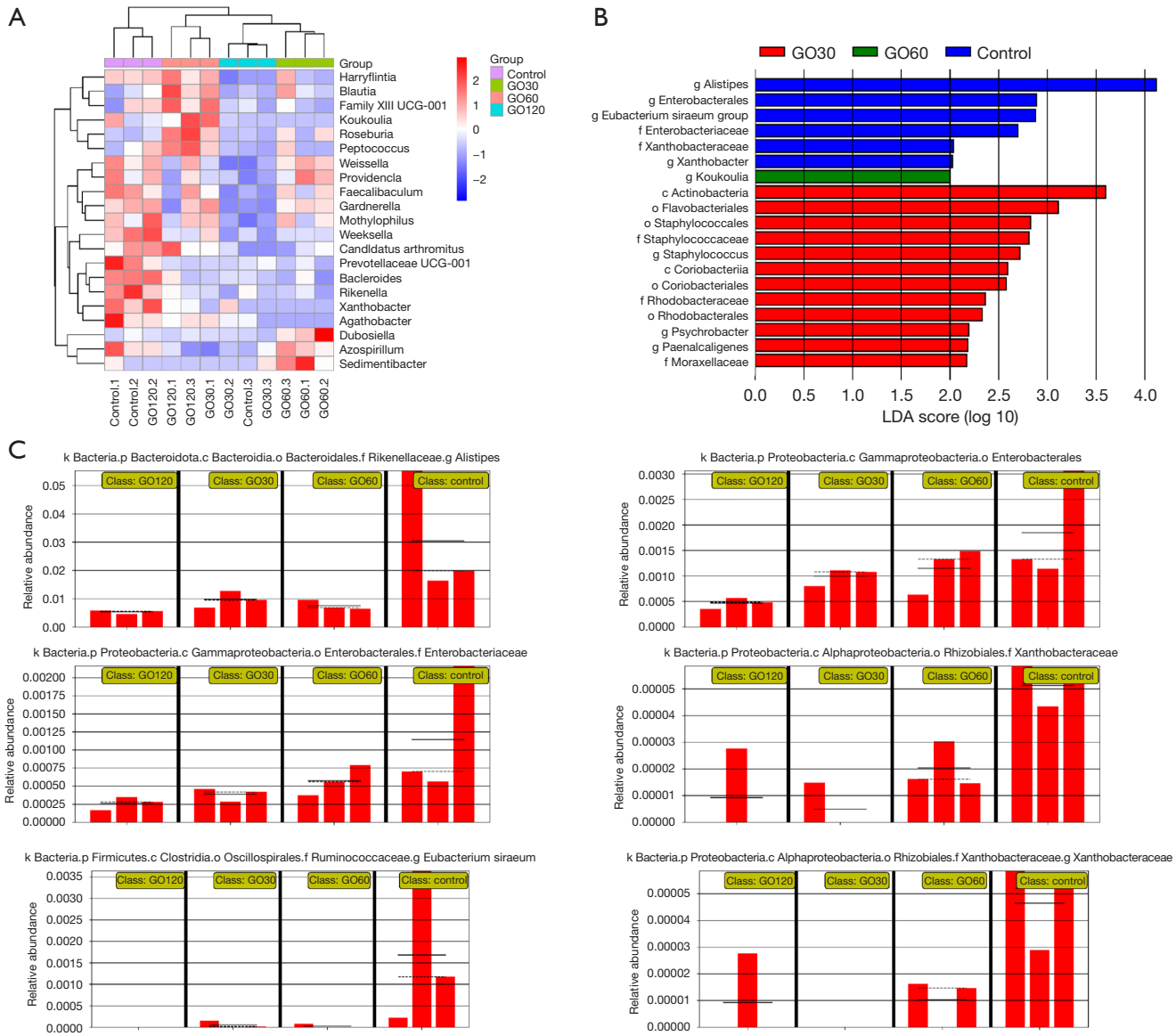

Figure 5 GO caused differences in microbial abundance between groups. (A) Heat maps of differential microorganisms at the genus level. (B) Score map of differential species. (C) Relative abundance of *Alistipes*, *Enterobacterales*, *Eubacterium siraeum*, *Enterobacteriaceae*, *Xanthobacteraceae*, and *Xanthobacter*. GO30, group with GO of dose 30 mg/kg; GO60, group with GO of dose 60 mg/kg; GO120, group with GO of dose 120 mg/kg; GO, graphene oxide; LDA, linear discriminant analysis.

diseases, such as ulcerative colitis and Crohn's disease. The damage of the intestinal ultrastructure directly destroys the integrity of the intestinal barrier. To further examine the changes of intestinal ultrastructure in mice induced by GO, TEM photographs were taken. The results showed that the intestinal ultrastructure of the 4 groups differed. In the control group, the intestinal barrier structure was complete, the connecting complex structure was present, and while the intercellular space was narrow, the epithelial organelles were not significantly swollen. In the GO30 and GO60 groups, the intestinal ultrastructure was slightly damaged, the connective complex structure remained, the local intercellular space was widened, and the epithelial cells showed slight edema. In the GO120 group, the intestinal ultrastructure was seriously damaged, the epithelial cell space was widened, and some cells showed a

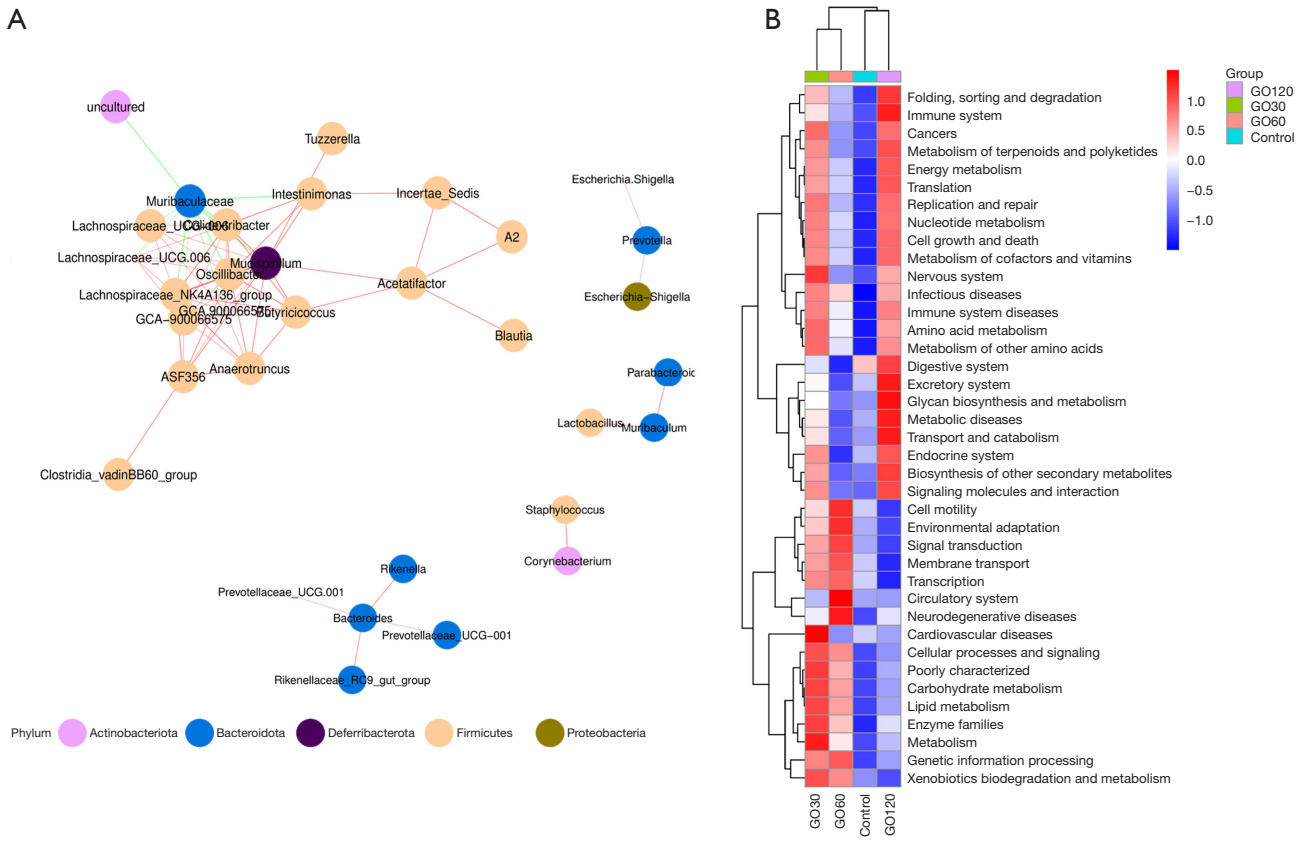

Figure 6 Prediction of GO's effects on the function of gut microbiota. (A) Correlation network analysis. (B) KEGG difference results on a clustering heatmap. GO30, group with GO of dose 30 mg/kg; GO60, group with GO of dose 60 mg/kg; GO120, group with GO of dose 120 mg/kg; GO, graphene oxide; KEGG, Kyoto Encyclopedia of Genes and Genomes.

tendency of apoptosis. These results indicate that GO can damage the intestinal ultrastructure and intestinal barrier. And this damage is positively correlated with increasing concentrations. This damage to the intestinal ultrastructure and the intestinal barrier poses a challenge to the safety of long-term oral preparations containing GO; thus, further modifications of GO are needed to weaken the damage to the intestinal barrier.

Gut microbiota is an important part of the human body, which is closely related to human health. The destruction and disturbance of the gut microbiota structure are relevant to many diseases, such as colitis and colon cancer. The results of this study showed that there was no significant difference in α diversity among the 4 groups. Conversely, the β diversity analysis showed significant differences, indicating that GO affected the diversity of flora among the groups. At the phylum level, we did not observe significant changes in the bacterial community structure. However, at the genus level, *Prevotellaceae*_UCG-001, *Alistipes*, and *Bacteroides* decreased in the GO group. And these decreases were positive correlated with increasing GO concentrations. Additionally, we also observed a decrease in the relative abundance of *Enterobacteriaceae* and *Eubacterium* in the GO group.

Alistipes is a relatively new genus in the phylum *Bacteroides*. It occupies a low proportion of the gut microbiota, but it is highly related to many diseases. Studies have shown that *Alistipes* is related to the pathogenesis of colorectal cancer, and is a potential pathogen (24,25). Moschen *et al.* showed that *Alistipes* promotes the occurrence of right colorectal cancer via the interleukin 6/signal transducer and activator of transcription 3 pathway (26). GO can reduce the level of *Alipipes*, indicating that oral administration of a certain dose of GO has potential benefits in preventing colorectal cancer.

The expansion of *Enterobacteriaceae* is closely related to

gastrointestinal inflammation (27). Many *Enterobacteriaceae* are facultative anaerobic bacteria, which consume oxygen to create an anaerobic environment conducive to the strict colonization of anaerobic bacteria (28), and lead to flora imbalance and inflammation. Several studies have observed a gut microbiota imbalance in inflammatory bowel disease (IBD) mouse models, and a greatly increased relative abundance of *Enterobacteriaceae* (29,30). Additionally, studies have also reported that *Enterobacteriaceae* is highly correlated with ulcerative colitis and Crohn's disease (31,32). GO reduces the level of *Enterobacteriaceae* in the gut microbiota of mice, which indicates that GO may have a preventive effect on the occurrence of IBD. However, previous study has also reported that the oral administration of GO can aggravate dextran sulfate sodium-induced colitis in mice (33). This may be related to the dose of GO and the intestinal state of mice, and further research needs to be conducted to clarify this issue.

Previous study has examined the gut microbiota of IBD patients, and found that the colonization of *Eubacterium* is reduced (34). *Eubacterium* can produce anti-cancer short-chain fatty acids. Thus, *Eubacterium* has always been considered to have a positive effect on the homeostasis of the intestine (35,36). However, Wang *et al.* showed that Eubacterium endotoxin can activate the transcription factor nuclear factor kappa-light-chain-enhancer of activated B cells, thereby promoting the occurrence of colitis, and leading to colon cancer (37). This study found contradicting results on the effects of Eubacterium on IBD and colorectal cancer that required further discussion.

Conclusions

In general, the study shows that oral GO had no obvious toxic effects on the hearts, livers, and kidneys of the mice, but affected the ultrastructure of the intestine and the structure of gut microbiota at higher concentrations of GO. As these effects may have some long-term negative consequences, the safety of oral GO administration needs to be further investigated.

Acknowledgments

Funding: This research was funded by the Natural Science Foundation of Minhang, Shanghai (No. 2021MHZ090) and the Medical System of Shanghai Minhang District (No. 2021MWDXK01).

Footnote

Reporting Checklist: The authors have completed the ARRIVE reporting checklist. Available at https://atm.amegroups.com/article/view/10.21037/atm-22-922/rc

Data Sharing Statement: Available at https://atm.amegroups.com/article/view/10.21037/atm-22-922/dss

Conflicts of Interest: All authors have completed the ICMJE uniform disclosure form (available at https://atm.amegroups.com/article/view/10.21037/atm-22-922/coif). The authors have no conflicts of interest to declare.

Ethical Statement: The authors are accountable for all aspects of the work in ensuring that questions related to the accuracy or integrity of any part of the work are appropriately investigated and resolved. Experiments were performed under a project license (No. m20210805) granted by Experimental Animal Welfare Ethics Committee of East China Normal University, in compliance with East China Normal University guidelines for the care and use of animals.

References

1. Novoselov KS, Geim AK, Morozov SV, et al. Electric field effect in atomically thin carbon films. Science 2004;306:666-9.
2. Stoller MD, Park S, Zhu Y, et al. Graphene-based ultracapacitors. Nano Lett 2008;8:3498-502.
3. Dreyer DR, Park S, Bielawski CW, et al. The chemistry of graphene oxide. Chem Soc Rev 2010;39:228-40.
4. Chung C, Kim YK, Shin D, et al. Biomedical applications of graphene and graphene oxide. Acc Chem Res 2013;46:2211-24.
5. Li R, Wang Y, Du J, et al. Graphene oxide loaded with

tumor-targeted peptide and anti-cancer drugs for cancer target therapy. Sci Rep 2021;11:1725.
6. Rahmanian N, Hamishehkar H, Dolatabadi JE, et al. Nano graphene oxide: a novel carrier for oral delivery of flavonoids. Colloids Surf B Biointerfaces 2014;123:331-8.
7. Pei X, Zhu Z, Gan Z, et al. PEGylated nano-graphene oxide as a nanocarrier for delivering mixed anticancer drugs to improve anticancer activity. Sci Rep 2020;10:2717.
8. Xia MY, Xie Y, Yu CH, et al. Graphene-based nanomaterials: the promising active agents for antibiotics-independent antibacterial applications. J Control Release 2019;307:16-31.
9. Narayanan KB, Park GT, Han SS. Antibacterial properties of starch-reduced graphene oxide-polyiodide nanocomposite. Food Chem 2021;342:128385.
10. Esmaeili Y, Bidram E, Zarrabi A, et al. Graphene oxide and its derivatives as promising In-vitro bio-imaging platforms. Sci Rep 2020;10:18052.
11. Torkashvand N, Sarlak N. Polymerized graphene oxide/MnCe0.5Fe1.5O4 nanoferrofluid as a T2- and T2*-weighted contrast agent for magnetic resonance imaging. Colloids Surf B Biointerfaces 2020;185:110555.
12. Sun N, Yin S, Lu Y, et al. Graphene oxide-coated porous titanium for pulp sealing: an antibacterial and dentino-inductive restorative material. J Mater Chem B 2020;8:5606-19.
13. Barrera CC, Groot H, Vargas WL, et al. Efficacy and Molecular Effects of a Reduced Graphene Oxide/Fe3O4 Nanocomposite in Photothermal Therapy Against Cancer. Int J Nanomedicine 2020;15:6421-32.
14. Deng X, Liang H, Yang W, et al. Polarization and function of tumor-associated macrophages mediate graphene oxide-induced photothermal cancer therapy. J Photochem Photobiol B 2020;208:111913.
15. Shamsi S, Alagan AA, Sarchio SNE, et al. Synthesis, Characterization, and Toxicity Assessment of Pluronic F127-Functionalized Graphene Oxide on the Embryonic Development of Zebrafish (Danio rerio). Int J Nanomedicine 2020;15:8311-29.
16. Priyadarsini S, Sahoo SK, Sahu S, et al. Oral administration of graphene oxide nano-sheets induces oxidative stress, genotoxicity, and behavioral teratogenicity in Drosophila melanogaster. Environ Sci Pollut Res Int 2019;26:19560-74.
17. Gurunathan S, Arsalan Iqbal M, Qasim M, et al. Evaluation of Graphene Oxide Induced Cellular Toxicity and Transcriptome Analysis in Human Embryonic Kidney Cells. Nanomaterials (Basel) 2019;9:969.
18. Yang K, Gong H, Shi X, et al. In vivo biodistribution and toxicology of functionalized nano-graphene oxide in mice after oral and intraperitoneal administration. Biomaterials 2013;34:2787-95.
19. Dreanca A, Sarosi C, Parvu AE, et al. Systemic and Local Biocompatibility Assessment of Graphene Composite Dental Materials in Experimental Mandibular Bone Defect. Materials (Basel) 2020;13:2511.
20. Pelin M, Sosa S, Prato M, et al. Occupational exposure to graphene based nanomaterials: risk assessment. Nanoscale 2018;10:15894-903.
21. Shao F, Hu N, Su Y, et al. Non-woven fabric electrodes based on graphene-based fibers for areal-energy-dense flexible solid-state supercapacitors. Chemical Engineering Journal 2019;392:123692.
22. Augustine R, Mamun AA, Hasan A, et al. Imaging cancer cells with nanostructures: Prospects of nanotechnology driven non-invasive cancer diagnosis. Adv Colloid Interface Sci 2021;294:102457.
23. Shamekhi MA, Mirzadeh H, Mahdavi H, et al. Graphene oxide containing chitosan scaffolds for cartilage tissue engineering. Int J Biol Macromol 2019;127:396-405.
24. Yang Y, Jobin C. Novel insights into microbiome in colitis and colorectal cancer. Curr Opin Gastroenterol 2017;33:422-7.
25. Parker BJ, Wearsch PA, Veloo ACM, et al. The Genus Alistipes: Gut Bacteria With Emerging Implications to Inflammation, Cancer, and Mental Health. Front Immunol 2020;11:906.
26. Moschen AR, Gerner RR, Wang J, et al. Lipocalin 2 Protects from Inflammation and Tumorigenesis Associated with Gut Microbiota Alterations. Cell Host Microbe 2016;19:455-69.
27. Baldelli V, Scaldaferri F, Putignani L, et al. The Role of Enterobacteriaceae in Gut Microbiota Dysbiosis in Inflammatory Bowel Diseases. Microorganisms 2021;9:697.
28. Arrieta MC, Stiemsma LT, Amenyogbe N, et al. The intestinal microbiome in early life: health and disease. Front Immunol 2014;5:427.
29. Yang I, Eibach D, Kops F, et al. Intestinal microbiota composition of interleukin-10 deficient C57BL/6J mice and susceptibility to Helicobacter hepaticus-induced colitis. PLoS One 2013;8:e70783.
30. Munyaka PM, Rabbi MF, Khafipour E, et al. Acute dextran sulfate sodium (DSS)-induced colitis promotes gut microbial dysbiosis in mice. J Basic Microbiol 2016;56:986-98.

31. Olbjørn C, Cvancarova Småstuen M, Thiis-Evensen E, et al. Fecal microbiota profiles in treatment-naïve pediatric inflammatory bowel disease - associations with disease phenotype, treatment, and outcome. Clin Exp Gastroenterol 2019;12:37-49.
32. Walujkar SA, Dhotre DP, Marathe NP, et al. Characterization of bacterial community shift in human Ulcerative Colitis patients revealed by Illumina based 16S rRNA gene amplicon sequencing. Gut Pathog 2014;6:22.
33. Liu S, Xu A, Gao Y, et al. Graphene oxide exacerbates dextran sodium sulfate-induced colitis via ROS/AMPK/p53 signaling to mediate apoptosis. J Nanobiotechnology 2021;19:85.
34. Guo X, Huang C, Xu J, et al. Gut Microbiota Is a Potential Biomarker in Inflammatory Bowel Disease. Front Nutr 2021;8:818902.
35. Pittayanon R, Lau JT, Leontiadis GI, et al. Differences in Gut Microbiota in Patients With vs Without Inflammatory Bowel Diseases: A Systematic Review. Gastroenterology 2020;158:930-946.e1.
36. Knoll RL, Forslund K, Kultima JR, et al. Gut microbiota differs between children with Inflammatory Bowel Disease and healthy siblings in taxonomic and functional composition: a metagenomic analysis. Am J Physiol Gastrointest Liver Physiol 2017;312:G327-39.
37. Wang Y, Wan X, Wu X, et al. Eubacterium rectale contributes to colorectal cancer initiation via promoting colitis. Gut Pathog 2021;13:2.

(English Language Editor: L. Huleatt)

Cite this article as: Shen J, Dong J, Zhao J, Ye T, Gong L, Wang H, Chen W, Fu M, Cai Y. The effects of the oral administration of graphene oxide on the gut microbiota and ultrastructure of the colon of mice. Ann Transl Med 2022;10(6):278. doi: 10.21037/atm-22-922

